


RESEARCH

Open Access



# Efficient delivery of mesenchymal stem/stromal cells to injured liver by surface PEGylation

Yukiya Takayama<sup>1,2†</sup>, Kosuke Kusamori<sup>1,3\*†</sup> , Yuri Katsurada<sup>1</sup>, Shu Obana<sup>1</sup>, Shoko Itakura<sup>1</sup> and Makiya Nishikawa<sup>1</sup>

## Abstract

**Background** Mesenchymal stem/stromal cells (MSCs) have been used in clinical trials for various diseases. These have certain notable functions such as homing to inflammation sites, tissue repair, and immune regulation. In many pre-clinical studies, MSCs administered into peripheral veins demonstrated effective therapeutic outcomes. However, most of the intravenously administered MSCs were entrapped in the lung, and homing to target sites was less than 1%. This occurred mainly because of the adhesion of MSCs to vascular endothelial cells in the lung. To prevent this adhesion, we modified the surface of MSCs with polyethylene glycol (PEG; a biocompatible polymer) using the avidin–biotin complex (ABC) method.

**Methods** The surface of MSCs was modified with PEG using the ABC method. Then, the cell adhesion to mouse aortic endothelial cells and the tissue distribution of PEG-modified MSCs were evaluated. Moreover, the homing to the injured liver and therapeutic effect of PEG-modified MSCs were evaluated using carbon tetrachloride-induced acute liver failure model mice.

**Results** The PEG modification significantly suppressed the adhesion of MSCs to cultured mouse aortic endothelial cells as well as the entrapment of MSCs in the lungs after intravenous injection in mice. PEG-modified MSCs efficiently homed to the injured liver of carbon tetrachloride-induced acute liver failure model mice. More importantly, the cells significantly suppressed serum transaminase levels and leukocyte infiltration into the injured liver.

**Conclusion** These results indicate that PEG modification to the surface of MSCs can suppress the lung entrapment of intravenously administered MSCs and improve their homing to the injured liver.

**Keywords** Cell surface modification, Liver failure, Lung entrapment, Mesenchymal stem/stromal cell, Polyethylene glycol

<sup>†</sup>Yukiya Takayama and Kosuke Kusamori contributed equally to this work.

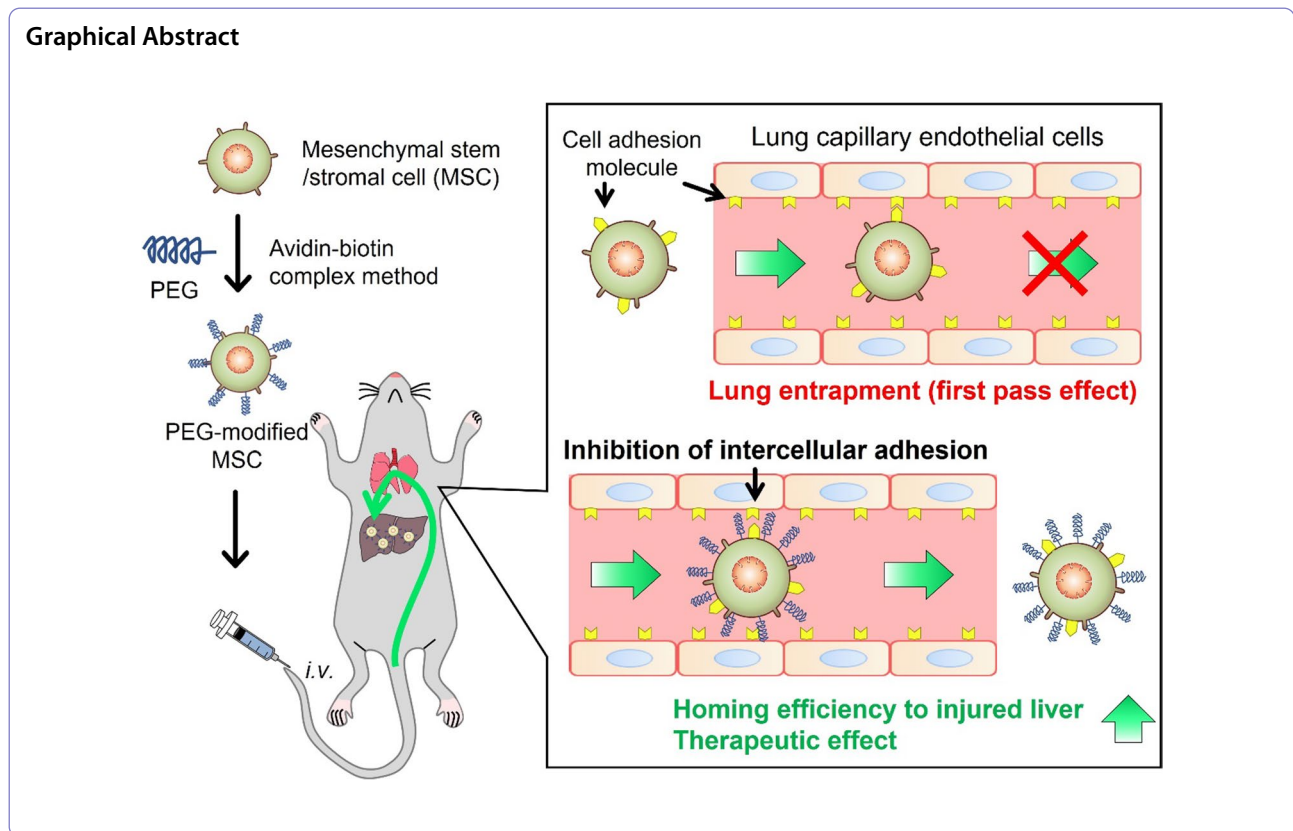
\*Correspondence:

Kosuke Kusamori

kusamori@rs.tus.ac.jp

Full list of author information is available at the end of the article





## Background

Mesenchymal stem/stromal cells (MSCs) are multipotent stem/progenitor cells. These can be isolated from various tissues including the bone marrow, adipose tissue, and umbilical cord [1–5]. After systemic administration, MSCs migrate to ischemic and inflammatory sites and exhibit immune regulatory and tissue repair activities by secreting cytokines, growth factors, and extracellular vesicles, as well as by direct cell-to-cell interactions [6, 7]. Furthermore, the high expandability and low immunogenicity of the cells enable the administration of autologous MSCs as well as allogeneic MSCs [5]. The number of clinical trials of MSCs is exponentially increasing worldwide. Most of these trials focus on the treatment of cardiovascular diseases, graft-versus-host disease, immune system diseases, wounds, and tissue restoration [8]. In addition, certain MSC products have been approved, including Prochymal and TEMCELL HS [9].

In many pre-clinical and clinical studies, MSCs are administered into peripheral veins because intravenous administration is a fundamental and minimally invasive administration method [10]. Furthermore, few adverse events have been reported in clinical studies in which MSCs were administered intravenously [10, 11]. However, the homing rate of intravenously administered MSCs to target sites was less than 1% [12]. This was

mainly because of their entrapment in the lung vasculature [13]. It is considered that the therapeutic mechanism of MSCs involves both paracrine effects [14–16] and cell-to-cell interactions in injured sites [17, 18]. Therefore, it is necessary to prevent lung entrapment and improve homing efficiency to target sites for effective MSC-based therapy. A few studies have reported that the interaction between cell adhesion molecules expressed on MSCs and vascular endothelial cells in the lung plays an important role in the lung entrapment of intravenously administered MSCs [19, 20]. The inhibition of this interaction suppressed the lung entrapment of MSCs. Kerkelä et al. [21] reported that the decomposition of cell membrane proteins of MSCs by pronase significantly suppressed lung entrapment. Wang et al. [22] obtained similar results by blocking integrins expressed on MSCs using monoclonal antibodies. However, these approaches may affect the homing of MSCs to target sites and their therapeutic efficiency. This is because the functions of cell membrane proteins are closely related to homing and cell-to-cell interactions. Therefore, the development of alternative approaches to prevent lung entrapment without significantly influencing the characteristics of MSCs (except for cell adhesion) is highly desirable.

Polyethylene glycol (PEG) is a biocompatible polymer that has been used frequently in the research field

pertaining to pharmaceutical sciences and cell engineering to improve the survival of transplanted cells by bypassing immune systems [23, 24]. Teramura et al. reported that cell surface modification with high molecular weight PEG (> 20 kDa; larger than the extracellular domains of cell adhesion molecules such as integrins) was effective for regulating the adhesion of L929 murine fibroblast cell line, human acute lymphoblastic leukemia T-cells, and human primary hepatocytes to scaffolds [25]. Therefore, PEG modification to the cell surface may be effective for preventing lung entrapment and improving the efficiency of homing to the target site of intravenously administered MSCs. However, conventional cell surface modification methods are generally toxic to MSCs because of unfavorable culture conditions in medium containing organic solvents for a long period [26]. To solve these disadvantages, we demonstrated earlier that cell surface modification using the avidin–biotin complex (ABC) method was effective for stable modification of MSCs with biotinylated and avidinated compounds in a short reaction time without significant modifications in the characteristics of MSCs [27, 28].

In this study, we modified the surface of MSCs with PEG using the ABC method and evaluated the effect of PEG modification on the lung entrapment and homing efficiency of MSCs to inflammation sites in mice. First, the surface of the murine mesenchymal stem cell line C3H10T1/2 cells was modified with PEG using the ABC method. Then, the influence of PEG modification on the characteristics of C3H10T1/2 cells was evaluated. Moreover, the cell adhesion to mouse aortic endothelial cells (MAECs) and the tissue distribution of intravenously administered PEG-modified C3H10T1/2 (PEG-C3H10T1/2) cells were evaluated. Finally, the homing to the injured liver and therapeutic effect of PEG-modified murine adipose-derived mesenchymal stem cell line m17.ASC (PEG-m17.ASC) cells were evaluated using carbon tetrachloride (CCl<sub>4</sub>)-induced acute liver failure model mice.

## Methods

### Materials

Isoflurane, streptavidin, 4% paraformaldehyde phosphate buffer solution, penicillin–streptomycin–L-glutamine solution, 0.4% trypan blue solution, sodium bicarbonate, Alizarin Red S (3,4-dihydroxy-9,10-dioxo-2-anthracenesulfonic acid sodium salt), Oil Red O (1-(2,5-dimethyl-4-(2,5-dimethylphenyl) phenyldiazonyl) azonaphthalen-2-ol), Triton X-100, bovine serum albumin, carbon tetrachloride (CCl<sub>4</sub>), olive oil, and transaminase CII-test Wako kit were purchased from FUJIFILM Wako Pure Chemical Co. (Osaka, Japan). A trypsin–EDTA solution (0.25% trypsin and 1 mM EDTA)

and antibiotic–antimycotic mixed stock solution (100×) were purchased from Nacalai Tesque Inc. (Kyoto, Japan). Dulbecco's modified Eagle's medium (DMEM) was purchased from Nissui Co., Ltd. (Tokyo, Japan). Claycomb medium, Medium 199, Hanks' balanced salt solution (HBSS), Alcian Blue staining solution, and carboxyfluorescein diacetate succinimidyl ester (CFSE) were purchased from Sigma-Aldrich Co. (St. Louis, MO, USA). Nunc Lab-Tek II Chamber Slides and Nunc Lab-Tek II Chambered Coverglasses were purchased from Thermo Fisher Scientific Inc. (Waltham, MA, USA). Fetal bovine serum (FBS) was purchased from Biosera (East Sussex, UK). Hygromycin B Gold was purchased from Invitrogen Life Technologies, Inc. (Carlsbad, CA, USA). Alexa Fluor 488 PEG Biotin (3400 Da, Alexa488-PEG-biotin) was purchased from Nanocs Inc. (New York, NY, USA). Anti-FAK (phospho Y397) antibody (anti-p-FAK IgG) was purchased from Abcam (Cambridge, UK). The O.C.T. compound was purchased from Sakura Finetechnical Co., Ltd. (Tokyo, Japan). Mesenchymal stem cell adipogenic differentiation medium, mesenchymal stem cell chondrogenic differentiation medium, and mesenchymal stem cell osteogenic differentiation medium were purchased from Clontech Laboratories Inc. (Mountain View, CA, USA). The Nano-Glo luciferase assay reagent was purchased from Promega Co. (Madison, WI, USA). Fluoromount-G was purchased from SouthernBiotech (Birmingham, AL, USA). VECTASHIELD Antifade Mounting Medium with DAPI was purchased from Vector Laboratories Inc. (Burlingame, CA, USA). Biotin-functionalized methoxy polyethylene glycol 2000 (PEG<sub>2k</sub>-biotin, 2000 Da) and biotin functionalized methoxy polyethylene glycol 20,000 (PEG<sub>20k</sub>-biotin, 20,000 Da) were purchased from Biopharma PEG Scientific Inc. (Watertown, MA, USA). All the other chemicals were of the highest commercially available grade.

### Cell culture

C3H10T1/2 cells were provided by Dr. Hiroki Kagawa (Department of Cell Biology, Kyoto Pharmaceutical University, Kyoto, Japan) and cultured in DMEM supplemented with 10% heat-inactivated FBS, 0.15% sodium bicarbonate, and 1% penicillin–streptomycin–L-glutamine solution. NanoLuc luciferase (NLuc)- and enhanced green fluorescent protein (GFP)-expressing C3H10T1/2 cells (C3H10T1/2/NLuc cells and C3H10T1/2/GFP cells, respectively) were cultured in DMEM supplemented with 10% heat-inactivated FBS, 0.15% sodium bicarbonate, 1% penicillin–streptomycin–L-glutamine solution, and 200 µg/mL hygromycin B. These cells were established in our previous reports [25]. m17.ASC cells were purchased from DS Pharma Biomedical (Osaka, Japan) and cultured in Claycomb

medium supplemented with 10% heat-inactivated FBS and 1% penicillin–streptomycin–L-glutamine solution. Nluc-expressing m17.ASC (m17.ASC/Nluc) cells (which were established in our previous reports [26]) were cultured in Claycomb medium supplemented with 10% heat-inactivated FBS, 1% penicillin–streptomycin–L-glutamine solution, and 200 µg/mL hygromycin B. MAECs were provided by Professor Ichiro Saito (Department of Pathology, Tsurumi University School of Dental Medicine, Yokohama, Japan) and cultured in Medium 199 supplemented with 10% heat-inactivated FBS and 1% antibiotic–antimycotic mixed stock solution.

#### Evaluation of cell surface modification with PEG

C3H10T1/2 cells ( $2 \times 10^5$  cells) were seeded into 100 mm cell culture dishes and incubated in a CO<sub>2</sub> incubator for 3 days. To modify the surface of C3H10T1/2 cells with PEG, C3H10T1/2 cells were detached from dishes using a trypsin–EDTA solution, washed two times with PBS, and collected in centrifuge tubes. The cells were then treated with 1 mM sulfo-NHS-LC-biotin for 20 min at room temperature, 50 µg/mL streptavidin for 10 min at 4 °C, and 100 µM PEG-biotin for 10 min at 4 °C. In each step, the cells were washed two times with PBS or HBSS. To verify the modification, streptavidin-modified C3H10T1/2 and unmodified C3H10T1/2 cells were incubated with 10 µM FITC-PEG-biotin for 10 min at 4 °C. After removing excess reagents by PBS wash, the cells were seeded onto Nunc Lab-Tek II Chamber Slide and incubated for 3 h in a CO<sub>2</sub> incubator. After incubation, the cells were fixed with 4% paraformaldehyde solution and observed under a confocal laser scanning microscope (TCS SP8, Leica Microsystem, Mannheim, Germany). In addition, after the FITC-PEG-biotin treatment, the cells were lysed using cell lysis buffer M, and the amount of PEG modified on the cells was determined by measuring the fluorescence intensity at an Ex/Em wavelength of 485/535 nm using a microplate reader (Wallac 1420 ARVO, PerkinElmer, Inc., Waltham, MA, USA). To evaluate the retention time of PEG modification, streptavidin-modified C3H10T1/2 cells were incubated with 50 µM Alexa488-PEG-biotin and seeded onto Nunc Lab-Tek II Chambered Coverglasses ( $1 \times 10^4$  cells/well). At 1, 3, and 6 h and 1, 2, 3, and 5 days after incubation, the cells were fixed with 4% paraformaldehyde solution and observed using a TCS SP8 confocal laser scanning microscope. In addition, Alexa488-PEG modified C3H10T1/2 cells were seeded into a 24-well culture plate, and the fluorescence intensity at an Ex/Em wavelength of 485/535 nm was measured using a Wallac 1420 ARVO microplate reader.

#### Characteristics of PEG-MSCs

To evaluate the cytotoxicity of PEG modification, the viability of PEG<sub>2k</sub>-modified C3H10T1/2 (PEG<sub>2k</sub>-C3H10T1/2) cells and PEG<sub>20k</sub>-modified C3H10T1/2 (PEG<sub>20k</sub>-C3H10T1/2) cells was evaluated using the trypan blue exclusion assay immediately after modification. PEG<sub>2k</sub>-C3H10T1/2 cells, PEG<sub>20k</sub>-C3H10T1/2 cells, and unmodified C3H10T1/2 cells were seeded into a 6-well culture plate ( $5 \times 10^4$  cells/well) to evaluate the cell proliferation of PEG-C3H10T1/2 cells. Furthermore, the number of cells was measured daily using the trypan blue exclusion assay. To evaluate cell differentiation, PEG<sub>2k</sub>-C3H10T1/2 cells, PEG<sub>20k</sub>-C3H10T1/2 cells, and unmodified C3H10T1/2 cells were cultured in adipogenic, osteogenic, or chondrogenic differentiation media according to the manufacturer's protocol. Furthermore, these were stained with Oil Red O, Alizarin Red S, and Alcian Blue staining solution, respectively, as reported previously [27].

#### In vitro adhesion assay

PEG<sub>2k</sub>-C3H10T1/2/Nluc cells, PEG<sub>20k</sub>-C3H10T1/2/Nluc cells, and unmodified C3H10T1/2/Nluc cells ( $2 \times 10^4$  cells/well) were seeded in a 96-well culture plate and incubated for 0.5, 1, 2, and 3 h in a CO<sub>2</sub> incubator. Then, nonadherent cells were removed by washing two times with PBS, and the number of adherent cells was evaluated by measuring the luciferase activity of the lysed cells using a Wallac 1420 ARVO microplate reader. To evaluate the adhesion of PEG-C3H10T1/2 cells to vascular endothelial cells, MAECs ( $2.5 \times 10^4$  cells/well) were seeded in a 96-well culture plate and incubated overnight in a CO<sub>2</sub> incubator. PEG<sub>2k</sub>-C3H10T1/2/Nluc cells, PEG<sub>20k</sub>-C3H10T1/2/Nluc cells, and unmodified C3H10T1/2/Nluc cells ( $2 \times 10^4$  cells/well) were seeded onto monolayered MAECs. Moreover, nonadherent C3H10T1/2/Nluc cells were removed by washing two times with PBS at 0.5, 1, 2, and 3 h after seeding. The number of C3H10T1/2/Nluc cells adhering to MAECs was determined by measuring the luciferase activity of the lysed cells. To observe PEG-C3H10T1/2 cells adhering to MAECs, MAECs ( $4 \times 10^4$  cells/well) were seeded onto Nunc Lab-Tek II Chambered Coverglasses and incubated overnight in a CO<sub>2</sub> incubator. PEG<sub>2k</sub>-C3H10T1/2/Nluc cells, PEG<sub>20k</sub>-C3H10T1/2/Nluc cells, and unmodified C3H10T1/2/Nluc cells ( $2 \times 10^4$  cells/well) were seeded onto monolayered MAECs and incubated for 2 h in a CO<sub>2</sub> incubator. Nonadherent C3H10T1/2/Nluc cells were removed by washing two times with PBS. Cells were fixed with 4% paraformaldehyde solution, mounted with VECTASHIELD Antifade Mounting Medium with DAPI, and observed using a digital microscope (BZ-9000, Keyence).

### Immunostaining

MAECs ( $4 \times 10^4$  cells/well) were seeded onto Nunc Lab-Tek II Chambered Coverglasses and incubated overnight in a CO<sub>2</sub> incubator. Then, PEG-modified or unmodified C3H10T1/2/GFP cells ( $1 \times 10^4$  cells/well) were seeded onto monolayered MAECs. The culture medium was removed 2 h after incubation, and the cells were incubated with 4% paraformaldehyde solution. Thirty minutes after incubation, 0.2% Triton X-100 in PBS and 1% bovine serum albumin in PBS were added to achieve permeabilization and blocking, respectively. The fixed cells were then incubated with anti-phospho-focal adhesion kinase (p-FAK) IgG primary antibody for 1 h at room temperature and stained with tetramethylrhodamine isothiocyanate (TRITC)-labeled secondary antibody for 1 h at room temperature. After immunostaining, the samples were mounted with Fluoromount-G and observed using a TCS P8 confocal laser scanning microscope. The fluorescence intensity of phospho-FAK observed in stained C3H10T1/2/GFP cells was measured by region of interest (ROI) analysis. Then, the average pixel intensity (pixel intensity per cell) of 15–20 randomly selected C3H10T1/2/GFP cells was calculated.

### Animals

Male C3H/He mice (4–8 weeks-old) were purchased from Sankyo Labo Service Co., Inc. (Tokyo, Japan). Male FVB mice (4–8 weeks-old) were purchased from CLEA Japan Inc. (Tokyo, Japan). The mice were maintained under specific pathogen-free (SPF) conditions. All the animal experiments were conducted in accordance with the principles and procedures outlined in the National Institutes of Health Guide for the Care and Use of Laboratory Animals. The protocols for the animal experiments were approved by the Animal Experimentation Committee of the Tokyo University of Science. All the mice were euthanized by cervical dislocation under isoflurane anesthesia.

### Tissue distribution of PEG-MSCs

To evaluate the tissue distribution of intravenously injected PEG-MSCs, PEG<sub>20k</sub>-C3H10T1/2/Nluc cells or unmodified C3H10T1/2/Nluc cells ( $1 \times 10^6$  cells/mouse in 100  $\mu$ L of PBS) were injected into the tail vein of C3H/He mice under isoflurane anesthesia. This experiment was conducted using 6 mice ( $n=3$  PEG<sub>20k</sub>-C3H10T1/2/Nluc group versus  $n=3$  unmodified C3H10T1/2/Nluc group). An hour after injection, blood was collected from the inferior vena cava under isoflurane anesthesia, and the mice were euthanized by cervical dislocation. Then, the organs were collected. The luciferase activity in the lysates of tissues and whole blood was measured as

reported previously [29]. In addition, to observe the cells in the lung, PEG-modified or unmodified C3H10T1/2 cells were labeled with CFSE as reported previously [30] and were injected into the tail vein of C3H/He mice under isoflurane anesthesia. An hour after injection, the lungs were excised from euthanized mice and fixed with 4% paraformaldehyde solution followed by embedding in O.C.T. compound. The lung samples were frozen using liquid nitrogen and sliced into 10- $\mu$ m-thick sections using a cryostat (CM3050 S, Leica Biosystems, Wetzlar, Germany). The tissue slides were observed under a BZ-9000 digital microscope. To evaluate the homing of MSCs to the injured liver, a CCl<sub>4</sub>-induced acute liver failure model was established by intraperitoneal injection of 1.5 mL/kg CCl<sub>4</sub> dissolved in olive oil (1:1 ratio) into FVB mice. Six hours after CCl<sub>4</sub> injection, PEG<sub>20k</sub>-m17.ASC/Nluc cells or unmodified m17.ASC/Nluc cells ( $1 \times 10^6$  cells/mouse in 100  $\mu$ L of PBS) were injected intravenously under isoflurane anesthesia. This experiment was conducted using 8 mice ( $n=4$  PEG<sub>20k</sub>-m17.ASC/Nluc group versus  $n=4$  unmodified m17.ASC/Nluc group). Twenty four hours after CCl<sub>4</sub> injection (18 h after m17.ASC/Nluc injection), the mice were euthanized by cervical dislocation, and the lungs and liver were collected. The luciferase activity in lysed tissues was measured as described above.

### Therapeutic effect of PEG-MSCs in CCl<sub>4</sub>-induced acute liver failure mice

To establish a CCl<sub>4</sub>-induced acute liver failure model, 1 mL/kg CCl<sub>4</sub> was intraperitoneally injected [31, 32] into FVB mice. The CCl<sub>4</sub> dose was determined in preliminary experiments. Six hours after CCl<sub>4</sub> injection, PBS, unmodified m17.ASC cells, or PEG<sub>20k</sub>-m17.ASC cells ( $1 \times 10^6$  cells/mouse in 100  $\mu$ L of PBS) were injected intravenously into mice under isoflurane anesthesia. Forty eight hours and 96 h after CCl<sub>4</sub> injection (42 h and 90 h after m17.ASC injection), blood was collected from the mice under isoflurane anesthesia, and these were euthanized by cervical dislocation. Serum was collected as reported previously [29], and serum aspartate aminotransferase (AST) and alanine aminotransferase (ALT) levels were measured using the transaminase CII-test Wako kit according to the manufacturer's protocol. For AST and ALT measurement after 48 h, 41 mice were used in the experiment ( $n=13$  CCl<sub>4</sub>-injured mice group versus  $n=14$  unmodified m17.ASC group versus  $n=13$  PEG<sub>20k</sub>-m17.ASC group). Two mice in the CCl<sub>4</sub>-injured mice group were excluded due to suspect of hemolysis of the blood samples during the blood sampling, and two mice in the PEG<sub>20k</sub>-m17.ASC group were excluded due to death of the mice. For AST and ALT measurement after 96 h, 28 mice were used in the experiment

( $n=4$  normal mice group versus  $n=8$   $\text{CCl}_4$ -injured mice group versus  $n=8$  unmodified m17.ASC group versus  $n=7$   $\text{PEG}_{20\text{k}}$ -m17.ASC group). One mouse in the  $\text{PEG}_{20\text{k}}$ -m17.ASC group was excluded due to death of the mouse. In addition, 96 h after  $\text{CCl}_4$  injection (90 h after m17.ASC injection), the liver was collected and embedded in O.C.T. compound, frozen, and cut into 10  $\mu\text{m}$  sections as described above. This experiment was conducted using 16 mice ( $n=4$  normal mice group versus  $n=4$   $\text{CCl}_4$ -injured mice group versus  $n=4$  unmodified m17.ASC group versus  $n=4$   $\text{PEG}_{20\text{k}}$ -m17.ASC group). The tissue slides were fixed with 4% paraformaldehyde solution and stained with hematoxylin and eosin according to a method published previously [33].

### Statistical analysis

Data were analyzed with the StatView software (SAS Institute, Inc., Cary, North Carolina, USA). A two-sided unpaired Student's *t*-test was used to evaluate statistically significant differences between groups. Meanwhile, multiple group comparisons were performed using one-way ANOVA followed by Bonferroni/Dunnnett's test. Differences were considered statistically significant when *p* values were less than 0.05.

## Results

### PEG modification of the surface of MSCs

To evaluate the cell surface modification with PEG, we selected FITC- or Alexa488-labeled PEG-biotin. The fluorescence intensity of FITC in FITC-PEG-modified C3H10T1/2 (FITC-PEG-C3H10T1/2) was significantly higher than that in FITC-PEG-biotin-treated unmodified C3H10T1/2 (FITC-PEG-biotin + C3H10T1/2) (Fig. 1A). In addition, confocal microscopic images showed that FITC fluorescence signals were localized on the surface of C3H10T1/2 cells (Fig. 1B). These results indicate that the surface of C3H10T1/2 cells was modified successfully with FITC-PEG-biotin using the ABC method. The retention time of PEG modification was evaluated using Alexa488-PEG-biotin (Fig. 1C, Additional file 1: Fig. S1). The fluorescence intensity of Alexa488-PEG decreased gradually in 24 h. It remained at 50% of the initial value after 120 h of incubation. Although certain fluorescence signals were detected inside C3H10T1/2 cells at subsequent time-points, the signals remained on the cell surface even on day 5. Furthermore, the influence of PEG modification on the characteristics of C3H10T1/2 cells was evaluated. PEG modification negligibly affected the viability, proliferation, and differentiation of C3H10T1/2 cells (Fig. 2).

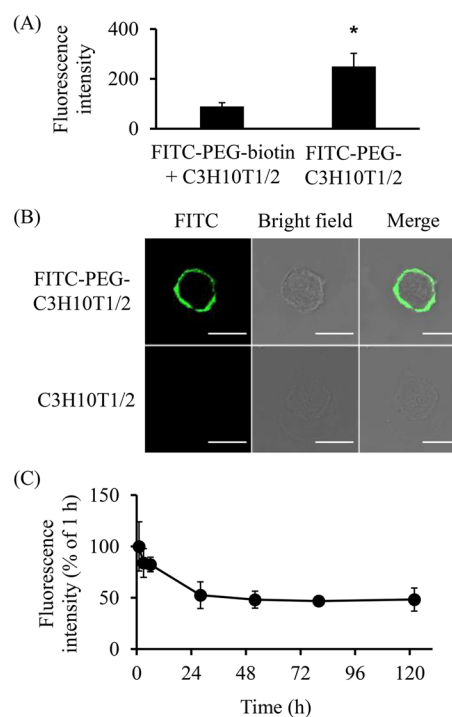


**Fig. 1** PEG modification to the surface of MSCs. **A** Fluorescence intensity of FITC-PEG-C3H10T1/2 cells. Streptavidin-modified C3H10T1/2 cells or unmodified C3H10T1/2 cells were incubated with FITC-PEG-biotin. The fluorescence intensity was measured using a microplate reader. The results are expressed as percentages of the value at 1 h. The error bars represent  $\pm$  SD,  $n=4$ , \* $p < 0.05$  versus FITC-PEG-biotin + C3H10T1/2 group. **B** Confocal imaging of FITC-PEG-C3H10T1/2 cells. Streptavidin-modified C3H10T1/2 cells or unmodified C3H10T1/2 cells were incubated with FITC-PEG-biotin. The cells were cultured for 3 h and observed using a confocal laser scanning microscope (scale bars: 20  $\mu\text{m}$ ). **C** Retention time of PEG modification. Streptavidin-modified C3H10T1/2 cells were incubated with Alexa488-PEG-biotin, and the fluorescence intensity was measured using a microplate reader. The error bars represent  $\pm$  SD,  $n=4$

### Inhibition of cell adhesion by PEG modification

The number of PEG-C3H10T1/2/Nluc cells was determined to evaluate the inhibitory effect of PEG modification on cell adhesion. The number of  $\text{PEG}_{2\text{k}}$ - and  $\text{PEG}_{20\text{k}}$ -C3H10T1/2/Nluc cells adhering to the culture plates was significantly lower than that of unmodified C3H10T1/2/Nluc cells (Fig. 3A). In addition, the number of  $\text{PEG}_{2\text{k}}$ - and  $\text{PEG}_{20\text{k}}$ -C3H10T1/2/Nluc cells adhering to MAECs was significantly lower than that of unmodified C3H10T1/2/Nluc cells (Fig. 3B). Furthermore, the inhibitory effect of  $\text{PEG}_{20\text{k}}$  modification was significantly higher than that of  $\text{PEG}_{2\text{k}}$  at 2 h and 3 h (Fig. 3B). Consistent with these results, microscopic observation showed that few  $\text{PEG}_{20\text{k}}$ -C3H10T1/2/

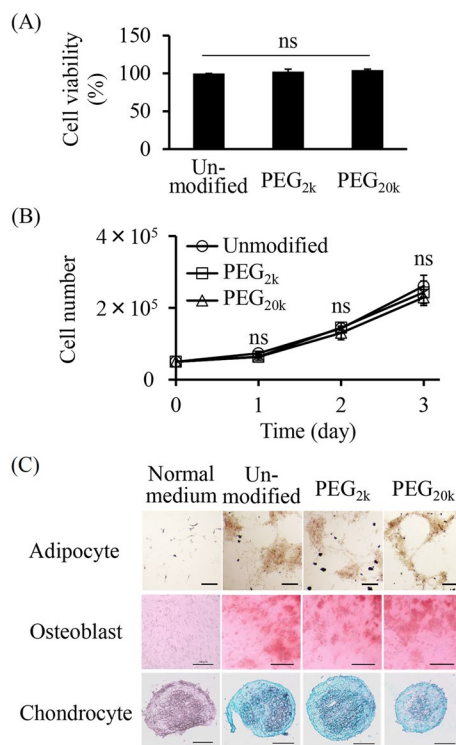


**Fig. 2** Characteristics of PEG-MSCs. **A** Cell viability of C3H10T1/2 cells after PEG modification. Streptavidin-modified C3H10T1/2 cells were incubated with PEG-biotin, and the cell viability was evaluated by trypan blue exclusion assay. The error bars represent  $\pm$  SD,  $n=4$  (*ns*; not significant). **B** Proliferation of PEG-C3H10T1/2 cells. The number of PEG-C3H10T1/2 cells or unmodified C3H10T1/2 cells was measured daily by trypan blue exclusion assay. The error bars represent  $\pm$  SD,  $n=4$  (*ns*; not significant). **C** Differentiation of PEG-C3H10T1/2 cells. Typical images of PEG-C3H10T1/2 cells and unmodified C3H10T1/2 cells differentiated into adipocytes, osteoblasts, or chondrocytes stained with oil red O, alizarin red S, and alcian blue, respectively (scale bars: 150  $\mu$ m)

Nluc cells bound to MAECs (Fig. 3C). The mixture of PEG-biotin and C3H10T1/2/Nluc cells and the cell surface modification with only biotin or streptavidin negligibly affected the adhesion of C3H10T1/2 cells to MAECs (Additional file 1: Fig. S2). We then evaluated the activation of integrins by immunostaining to investigate whether PEG modification inhibits the interaction between cell adhesion molecules of C3H10T1/2 cells and MAECs. Integrins play important roles in cell adhesion. Immunostaining showed that PEG modification markedly suppressed the activation of FAK (a key mediator of intracellular signaling by integrins) at 2 h after seeding C3H10T1/2 cells. This indicates that PEG modification inhibited the activation of integrins in C3H10T1/2 cells (Fig. 3D, E). In addition, the PEG-modified cells were not spindle-shaped, indicating weak cell adhesion compared with unmodified C3H10T1/2

cells (Fig. 3D). Meanwhile, 12 h after seeding, no significant differences were observed in the adhesion of C3H10T1/2 cells to MAECs in any of the groups examined (Additional file 1: Fig. S3). These results indicate that PEG modification of the surface of MSCs using the ABC method temporally suppressed intercellular adhesion between MSCs and vascular endothelial cells. Because PEG<sub>20k</sub> was better than PEG<sub>2k</sub> in suppressing the adhesion of C3H10T1/2 cells to MAECs, PEG<sub>20k</sub> was used for PEG modification in the following studies.

#### Tissue distribution of PEG-MSCs after intravenous administration

The tissue distribution of PEG-C3H10T1/2 cells in C3H/He mice was evaluated to determine the effect of PEG modification on lung entrapment of intravenously injected MSCs. PEG<sub>20k</sub>-C3H10T1/2/Nluc cells or unmodified C3H10T1/2/Nluc cells were injected into the tail vein of C3H/He mice. One hour after injection, the number of PEG<sub>20k</sub>-C3H10T1/2/Nluc cells in the lung was significantly lower than that of unmodified C3H10T1/2/Nluc cells (Fig. 4A). Moreover, the number of PEG<sub>20k</sub>-C3H10T1/2/Nluc cells in the liver was significantly higher than that of unmodified C3H10T1/2/Nluc cells. Consistent with this outcome, the number of CFSE-labeled PEG<sub>20k</sub>-C3H10T1/2 cells in lung tissue sections was lower than that of CFSE-labeled C3H10T1/2 cells (Fig. 4B). These results indicate that PEG<sub>20k</sub> modification to the surface of MSCs using the ABC method suppressed the lung entrapment of intravenously administered MSCs by preventing intercellular adhesion between MSCs and vascular endothelial cells in the lung. Then, the homing efficiency of intravenously injected PEG-MSCs to inflammation sites was evaluated using a CCl<sub>4</sub>-induced acute liver failure model (which is commonly used to evaluate MSC homing [34–36]) and m17.ASC cells (which showed a high homing capability to an injured liver in a previous study [37]). Six hours after CCl<sub>4</sub> injection, the serum AST and ALT levels in the CCl<sub>4</sub>-injured mice group were significantly higher than those in the vehicle-treated group (Additional file 1: Fig. S4). Based on these results, m17.ASC cells were injected 6 h after CCl<sub>4</sub> injection, and their homing to the injured liver was evaluated 24 h after injection (Fig. 4C). This approach was adopted because certain studies reported that intravenously administered MSCs can be detected in the liver several hours after MSC administration [5, 35, 38]. The number of PEG<sub>20k</sub>-m17.ASC/Nluc cells in the injured liver was significantly higher than that in the unmodified m17.ASC/Nluc cells (Fig. 4D). These results indicate that PEG<sub>20k</sub> modification to the surface of m17.ASC cells

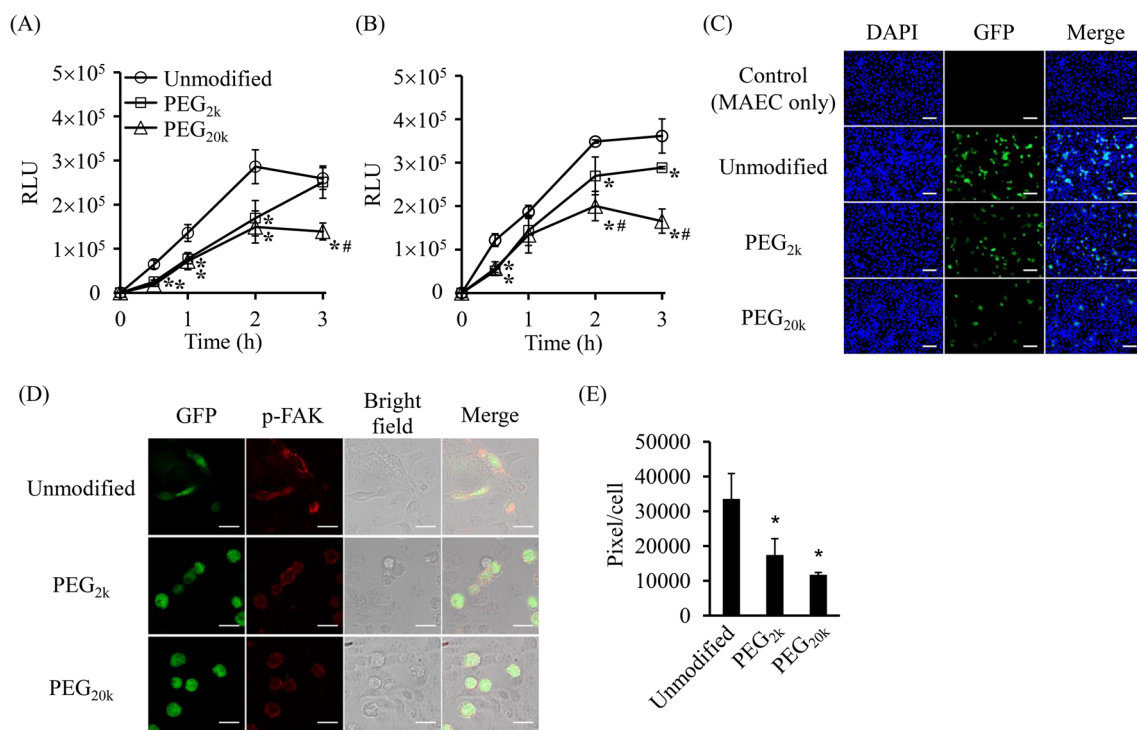


**Fig. 3** Inhibition of cell adhesion by PEG modification. **A** Number of C3H10T1/2 cells adhering to a culture plate. Unmodified or PEG-C3H10T1/2/Nluc cells were seeded onto a culture plate, and nonadherent cells were removed by PBS wash. The adhering cells were evaluated by measuring the luciferase activity. The error bars represent  $\pm$ SD,  $n=4$ , \* $p < 0.05$  versus unmodified group, # $p < 0.05$  versus PEG<sub>2k</sub> group. **B, C** Adhesion of C3H10T1/2 cells to monolayered MAECs. Unmodified or PEG-C3H10T1/2 cells were seeded onto monolayered MAECs, and nonadherent C3H10T1/2 cells were removed by PBS wash. The adhering cells were evaluated by measuring the luciferase activity of C3H10T1/2/Nluc cells (**B**). Two hours after seeding, adhering C3H10T1/2/GFP cells were observed using a fluorescence microscope (**C**). The error bars represent  $\pm$ SD,  $n=4$ , \* $p < 0.05$  versus unmodified group, # $p < 0.05$  versus PEG<sub>2k</sub> group (scale bars: 100  $\mu$ m). **D, E** Immunofluorescence staining for p-FAK in C3H10T1/2/GFP cells. Unmodified or PEG-C3H10T1/2/GFP cells were seeded onto monolayered MAECs. Two hours after incubation, cells were stained and observed using a confocal laser scanning microscope (**D**). Furthermore, the fluorescence intensity from p-FAK was measured by ROI analysis (**E**). The error bars represent  $\pm$ SD,  $n=3$ , 15–20 cells analyzed per sample, \* $p < 0.05$  versus unmodified group (scale bars: 20  $\mu$ m)

suppressed lung entrapment and improved homing to the injured liver after intravenous injection.

#### Therapeutic effect of PEG-MSCs in acute liver failure model mice

The therapeutic effect of intravenously injected PEG-m17.ASC cells was evaluated using the CCl<sub>4</sub>-induced acute liver failure model (Fig. 5A). Forty eight hours after CCl<sub>4</sub> injection, the serum AST levels of the unmodified m17.ASC group and PEG<sub>20k</sub>-m17.ASC group were significantly lower ( $p < 0.05$  and  $p < 0.01$ , respectively) than that of the CCl<sub>4</sub>-injured mice group (Fig. 5B). The serum ALT level was also significantly lower ( $p < 0.01$ ,  $p < 0.001$ , respectively). Ninety six hours after CCl<sub>4</sub> injection, the serum AST levels of the unmodified m17.ASC group and PEG<sub>20k</sub>-m17.ASC group were significantly lower ( $p < 0.01$  and  $p < 0.001$ , respectively) than that of the CCl<sub>4</sub>-injured mice group. The serum ALT level was also significantly lower ( $p < 0.05$ ,  $p < 0.01$ , respectively). Furthermore, leukocyte infiltration in the injured liver of the unmodified

and PEG<sub>20k</sub> groups was significantly lower than that in the CCl<sub>4</sub>-injured mice group (Fig. 5C, D). Overall, the PEG<sub>20k</sub> group showed superior therapeutic effects compared with the unmodified group. These results indicate that PEG<sub>20k</sub> modification to the surface of MSCs improved the homing efficiency to the inflammation sites and the therapeutic effect of intravenously administered MSCs.

#### Discussion

Modifying cell surface properties to prevent lung entrapment of MSCs after intravenous injection can be a key technique for successful systemic MSC-based therapy. A few clinical studies have demonstrated that intravenous administration of MSCs exhibits effective therapeutic outcomes against diseases such as acute myocardial infarction, type 2 diabetes, diabetic nephropathy, rheumatoid arthritis, acute graft-versus-host disease, and coronavirus disease (COVID-19) [10, 11, 39, 40]. Although the therapeutic mechanism of MSCs is considered to



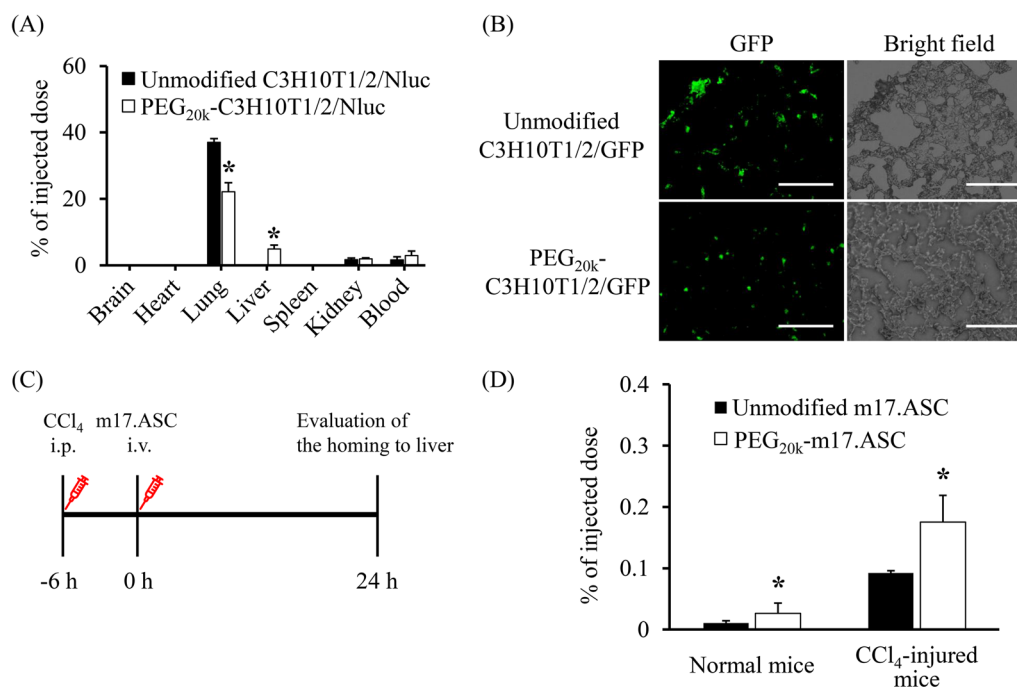


**Fig. 4** Inhibition of lung entrapment and improvement of homing efficiency of MSCs by PEG modification. **A** Tissue distribution of intravenously injected unmodified and PEG<sub>20k</sub>-C3H10T1/2 cells in normal mice. Unmodified or PEG<sub>20k</sub>-C3H10T1/2/Nluc cells were injected into the tail vein of C3H/He mice. One hour after injection, the organs and blood were collected, and the luciferase activity was measured. The error bars represent  $\pm$ SD,  $n=3$ , \* $p < 0.05$  versus unmodified group. **B** Typical images of lung tissue section. Frozen lung sections were observed 1 h after injection of CFSE-labeled unmodified or PEG<sub>20k</sub>-C3H10T1/2 cells (scale bars: 100  $\mu$ m). **C**, **D** Homing of m17.ASC cells to injured liver in CCl<sub>4</sub>-induced acute liver failure model mice. **C** Schematic image of experimental design. Schematic created with Microsoft PowerPoint. **D** The luciferase activity in the liver was measured 24 h after intravenous injection of unmodified or PEG<sub>20k</sub>-m17.ASC/Nluc cells to normal or CCl<sub>4</sub>-injured FVB mice. The error bars represent  $\pm$ SD,  $n=4$ , \* $p < 0.05$  versus unmodified group

involve paracrine effects and cell-to-cell interactions [6, 16, 17], the homing efficiency of intravenously administered MSCs to the target site is low. This indicates that MSCs do not fully exert their therapeutic potential. In the present study, the surfaces of MSCs were modified with PEG using the ABC method to improve the homing efficiency to the inflammation sites after intravenous injection. PEG modification temporarily suppressed the adhesion of C3H10T1/2 cells to MAECs and suppressed lung entrapment after intravenous injection of C3H10T1/2 cells. Furthermore, the homing efficiency and therapeutic effect of m17.ASC cells were improved by PEG modification. Therefore, PEG modification would be effective to improve the homing efficiency and therapeutic efficacy of MSCs by preventing lung entrapment.

Conventional cell surface modification with polymers (e.g., hydrophobic insertion of lipid conjugates and layer formation with charged polymers) causes cell membrane damage by long-term incubation with organic solvent-containing media [26]. Cell surface modification using the ABC method can rapidly and stably modify the cell surface with avidinated or biotinylated compounds under organic solvent-free conditions. These suitable conditions

enable the modification of the surface of MSCs with minimum cytotoxicity [27]. In the present study, streptavidin-modified C3H10T1/2 cells were modified successfully with PEG-biotin after 10 min of incubation (Fig. 1A, B) without significant variations in the viability, proliferation, or differentiation capability (Fig. 2). In addition, PEG-C3H10T1/2 cells were differentiated into chondrocytes (Fig. 2C) which require cell–cell interaction in the differentiation process. This may be because the inhibitory effect of PEG modification on cell adhesion decreased with time in accordance with the internalization of PEG into the cytoplasm (Additional file 1: Fig. S1).

The molecular weight and other physicochemical properties of the compounds modified on the cell surface are important for the function of surface-modified cells. Teramura et al. reported that high molecular weight PEG (>20 kDa; larger than certain cell adhesion molecules such as integrins) affected the cellular adhesion of PEG-modified cells. However, low molecular weight (2 kDa or 5 kDa) PEG had a negligible effect [25]. In the present study, 2 kDa PEG (PEG<sub>2k</sub>) and 20 kDa PEG (PEG<sub>20k</sub>) were used to investigate the effect of PEG chain length on the adhesion of C3H10T1/2 cells to endothelial cells.

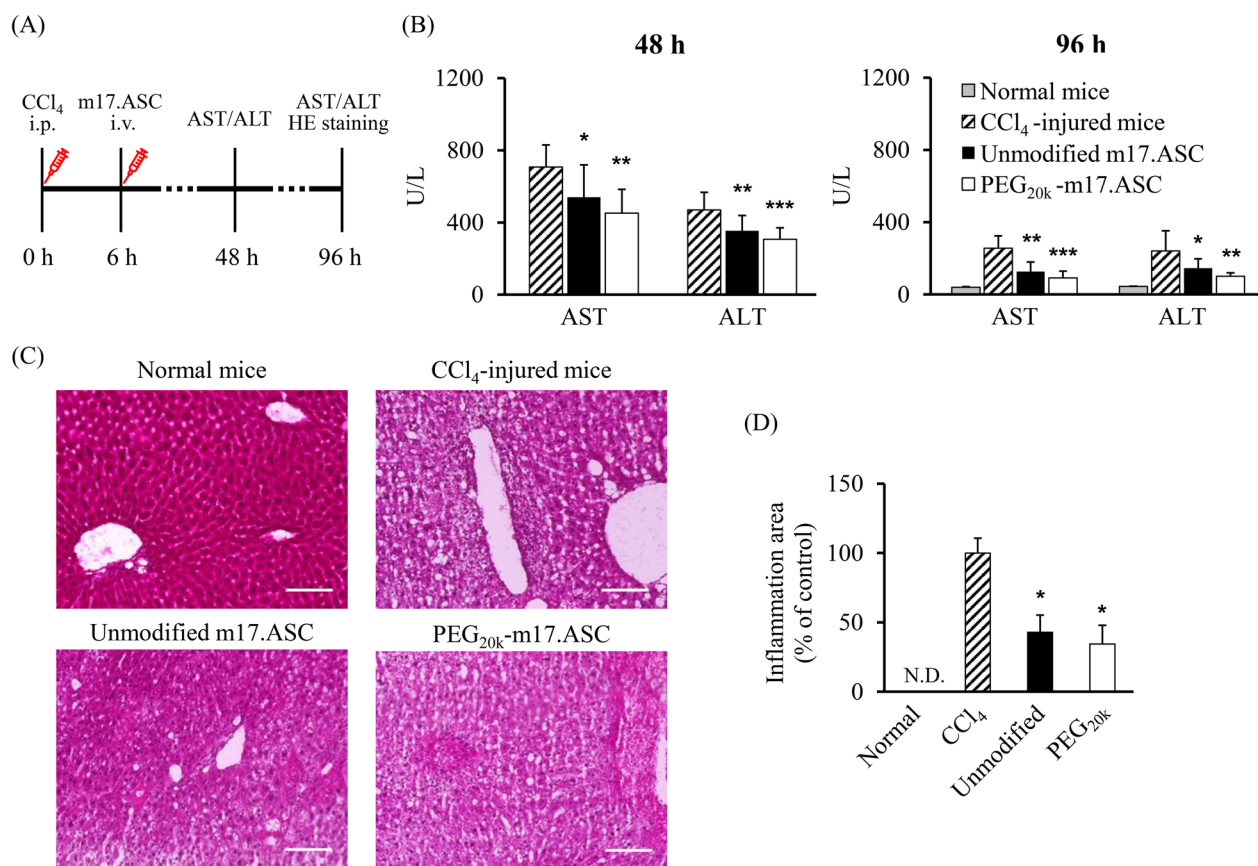


**Fig. 5** Therapeutic effect of PEG-MSCs in CCl<sub>4</sub>-induced acute liver failure model mice. **A** Schematic image of the experimental design. Schematic created with Microsoft PowerPoint. **B** Serum AST and ALT levels of acute liver failure model mice treated with PEG-m17.ASC cells. The serum AST and ALT levels were measured 48 h and 96 h after CCl<sub>4</sub> injection (42 h and 90 h after m17.ASC injection). The normal mice group was administered neither CCl<sub>4</sub> nor m17.ASC cells. The CCl<sub>4</sub>-injured mice group was administered only CCl<sub>4</sub>. The error bars represent  $\pm$ SD,  $n=4-14$ , \* $p < 0.05$ , \*\* $p < 0.01$ , \*\*\* $p < 0.001$  versus CCl<sub>4</sub>-injured mice group. **C, D** Anti-inflammatory effect of PEG<sub>20k</sub>-m17.ASC cells. Ninety six hours after CCl<sub>4</sub> injection (90 h after m17.ASC injection), the liver section was stained with hematoxylin and eosin (**C**). Furthermore, the inflammation area accompanying the leucocyte infiltration was measured by ROI analysis (**D**). The normal mice group was administered neither CCl<sub>4</sub> nor m17.ASC cells. The CCl<sub>4</sub>-injured mice group was administered only CCl<sub>4</sub>. The error bars represent  $\pm$ SD,  $n=4$ , \* $p < 0.05$  versus CCl<sub>4</sub>-injured mice group (scale bars: 100  $\mu$ m. N.D. not detected)

Since PEG<sub>20k</sub> showed more pronounced effects than PEG<sub>2k</sub> (Fig. 3A, B), we found that the PEG chain length was critical for cell adhesion. However, in our previous study, cell surface modification with Nluc (19 kDa) negligibly affected the cell adhesion of MSCs [27]. Yao et al. [41] reported that avidin (66 kDa) modification negligibly affected the cellular characteristics of MSCs. Similarly, streptavidin (55 kDa) modification did not significantly affect the cell adhesion of C3H10T1/2 cells (Additional file 1: Fig. S2)). These results indicate that PEG exhibits properties different from those of other macromolecular compounds on the surface of modified cells. PEG is widely used for surface modification of nanoparticles to prevent phagocytosis by mononuclear phagocytes [42]. PEG is a highly hydrophilic polymer, and PEG modification is considered to form an aqueous layer on the surface

of nanoparticles [42]. Based on these characteristics, cell surface modification with PEG<sub>20k</sub>, but not with PEG<sub>2k</sub>, could efficiently inhibit the adhesion of C3H10T1/2 cells to endothelial cells by covering cell membrane proteins such as cell adhesion molecules.

Although many studies have shown the regulation of in vitro cell adhesion by cell surface modification, there are few reports demonstrating in vivo results on the regulation of cell adhesion by cell surface modification with polymers, particularly with PEG [21, 22, 25, 43–52]. In the present study, we demonstrated that PEG modification was effective for preventing lung entrapment of intravenously administered MSCs (Fig. 4B, C). However, the avoidance was incomplete. There are several factors that affect lung entrapment, including the size of MSCs [13], thrombus formation [34, 51–54], and

intercellular adhesion between MSCs and endothelial cells in the lung [20–22]. It is necessary to control these factors simultaneously to achieve further reduction in lung entrapment. As shown in Fig. 4A, the total number of PEG<sub>20k</sub>-C3H10T1/2/Nluc cells (31.9%) detected in major organs and whole blood was lower than that of unmodified C3H10T1/2/Nluc cells (40.5%). This could be owing to the distribution of the cells to the unevaluated organs and tissues (e.g., brain, intestine, and muscle). On the other hand, some studies demonstrated that PEG modification improved the engraftment of islets by bypassing host immune systems [24, 55–62]. Therefore, improved survival of MSCs by PEG modification may increase the therapeutic effect after transplantation.

MSCs adhere to blood endothelial cells via various cell adhesion molecules [7]. In particular, integrins play an important role in cell adhesion between MSCs and blood endothelial cells in the lung vessel [22], and the PEG modification significantly inhibited the activation of integrins in C3H10T1/2 cells in vitro (Fig. 3D, E). These data suggest that the adhesion inhibitory effect by the PEG modification is due to the suppression of interaction between adhesion molecules of MSCs and endothelial cells. On the other hand, the in vivo adhesion between MSCs and endothelial cells takes place in a blood stream which is a dynamic environment. Some studies developed in vitro flow adhesion assay systems and demonstrated the strength of adhesion and steps of extravasation under physiological flow conditions [42, 59–62]. In the present study, PEG modification suppressed the adhesion of C3H10T1/2 cells to MAECs under an in vitro static condition and the entrapment of C3H10T1/2/Nluc cells in the lungs of mice (Figs. 3B, 4A). According to these results, the influence of the PEG modification on the lung entrapment of intravenously administered MSCs could be predicted by the simple and static experimental condition. Wang et al. [21] also succeeded in evaluating the influence of integrin antibodies for the lung entrapment of intravenously administered MSCs under an in vitro static experimental condition.

There are multiple processes in the homing of MSCs, such as chemokine-triggered activation, surface molecule-mediated rolling and adhesion to the endothelium, and transendothelial migration [13]. As shown in Fig. 4D, PEG modification significantly improved the homing efficiency of m17.ASC cells to the injured liver. This indicates that PEG modification negligibly affected the homing capability of MSCs to injured sites. In addition, the amount of PEG modified on the cell surface is important for the homing capability of MSCs. Although high-density or multiple layers coating of cell surface with polymers [63, 64] could inhibit the chemokine-triggered activation, in our previous study, cell surface

modification with liposomes by the ABC method did not affect the migratory potency of MSCs due to low occupation (3.6% of the cell surface) [29]. Furthermore, the PEG modified on the cell surface decreased gradually and that the inhibitory effect of PEG on cell adhesion could weaken with time. The in vitro results (Fig. 1C) support this hypothesis. Furthermore, micropinocytosis (which is activated by chemokines [65]) may enhance PEG internalization, and the inhibiting effect may be reduced near the inflammation sites.

Considering the tissue distribution of PEG-modified MSCs, the distribution of PEG-modified MSCs to the liver dramatically increased in normal mice compared to that of unmodified MSCs (Fig. 4A), showing MSCs may be more likely to distribute to the liver, which is a large organ with rich blood flow and capillaries, after passing through the lung. In addition, the distribution of PEG-modified MSCs to the injured liver increased more (Fig. 4D), probably because of the homing ability of MSCs to injured sites. About the distribution to the other tissues, the remaining of PEG-modified MSCs in the blood increased 1 h after intravenous administration, but that to the other organs hardly changed (Fig. 4A), suggesting that PEG-modified MSCs escaped from lung entrapment, remained in the blood, and reaching mainly the liver. On the other hand, PEG-modified MSCs may not recognize the adhesion molecules in the injured liver. In this point as described above, the PEG modification on the cell surface gradually decreases, and the inhibitory effect of PEG on cell adhesion may become weakened with time. Thus, PEG modified on MSCs may temporarily suppress the lung entrapment, and then allow MSCs to interact with adhesion molecules in injured liver as PEG is gradually removed from cells.

Many studies have reported that a majority of intravenously administered MSCs are entrapped in the lung [13]. However, few attempts have been undertaken to prevent this entrapment and improve delivery efficiency to target sites [21, 22]. It is becoming increasingly evident that the main therapeutic mechanism of intravenously injected MSCs is paracrine effects or apoptosis in MSCs rather than differentiation into damaged cells [10, 66, 67]. Certain studies reported that although intravenously injected MSCs were distributed mainly in the lung, the inflammatory reaction was alleviated in liver failure model mice [15], drug-induced nephropathy model mice [68], and pancreatitis model mice [69]. These studies indicated that secretomes from MSCs in the lungs show immune regulatory and tissue repair effects. However, certain groups recently reported that direct cell-to-cell interactions at the inflammation site are also important for immune regulatory and tissue repair effects of MSCs [17, 18]. Furthermore, although over 1000 clinical trials

relevant to MSCs are registered on FDA.gov, many trials in large stages showed negligible therapeutic effect [11]. Furthermore, no MSC product was approved by the Food and Drug Administration (FDA) as of September 2021. In the present study, the improved homing efficiency demonstrated the higher therapeutic efficiency of intravenously administered m17.ASC cells. This indicates the importance of regulating the biodistribution of intravenously administered MSCs to achieve effective MSC-based therapy.

## Conclusion

MSCs were successfully modified with PEG using the ABC method without cell damage, and PEG modification prevented lung entrapment of intravenously administered MSCs. Furthermore, PEG modification improved the homing efficiency to the injured liver of CCl<sub>4</sub>-induced acute liver failure model mice, and intravenously injected PEG-MSCs suppressed serum transaminase levels and leukocyte infiltration in the injured liver. These results indicate that cell surface modification with PEG may be an effective engineering procedure for effective MSC-based therapy.

## Abbreviations

ABC	Avidin–biotin complex
ALT	Alanine aminotransferase
AST	Aspartate aminotransferase
NLuc	NanoLuc luciferase
C3H10T1/2	Murine mesenchymal stem cell line
CCl <sub>4</sub>	Carbon tetrachloride
CFSE	Carboxyfluorescein diacetate succinimidyl ester
COVID-19	Coronavirus disease
FBS	Fetal bovine serum
HGF	Hepatocyte growth factor
MAECs	Mouse aortic endothelial cells
MSCs	Mesenchymal stem/stromal cells
m17.ASC	Murine adipose-derived mesenchymal stem cell line
PEG	Polyethylene glycol
p-FAK	Phospho-focal adhesion kinase
ROI	Region of interest
SPF	Specific pathogen-free
TRITC	Tetramethylrhodamine isothiocyanate

## Supplementary Information

The online version contains supplementary material available at <https://doi.org/10.1186/s13287-023-03446-w>.

**Additional file 1.** Supplementary figures.

## Acknowledgements

We wish to thank Kodai Takamura and Kazuma Nishimura (Laboratory of Biopharmaceutics, Faculty of Pharmaceutical Sciences, Tokyo University of Science, Noda, Chiba, Japan) for their kind support in certain experiments and Editage ([www.editage.com](http://www.editage.com)) for their English language editing.

## Author contributions

YT: methodology, investigation, writing (original draft). KK: investigation, conceptualization, formal analysis, validation, writing, review, and editing. YK:

investigation. SO: investigation. SI: writing, review, and editing. MN: methodology, validation, formal analysis, writing, review, and editing. All authors read and approved the final manuscript.

## Funding

This work was supported in part by a Grant-in-Aid for Young Scientists B (Grant Number 15K18850) and Grant-in-Aid for JSPS Fellows (20J14253) from the Japan Society for the Promotion of Science (JSPS), a grant from Inohana Shogakukai, and a grant from the Foundation for Interaction in Science & Technology (FIST).

## Availability of data and materials

The dataset supporting the conclusions of this article is included within the article and its additional file.

## Declarations

### Ethics approval and consent to participate

The protocols for the animal experiments were approved by the Animal Experimentation Committee of the Tokyo University of Science. Title of the approved project, Preparation of pathological animal models and evaluation of cellular functions by cell transplantation into rodents; Approval number, Y22016; Date of approval, May 9, 2022.

### Consent for publication

Not applicable.

### Competing interests

The authors declare that they have no competing interests.

### Author details

<sup>1</sup>Laboratory of Biopharmaceutics, Faculty of Pharmaceutical Sciences, Tokyo University of Science, 2641 Yamazaki, Noda, Chiba 278-8510, Japan. <sup>2</sup>Department of Pharmacy, Kobe City Hospital Organization, Kobe City Medical Center General Hospital, Chuo-Ku, Kobe 650-0047, Japan. <sup>3</sup>Laboratory of Cellular Drug Discovery and Development, Faculty of Pharmaceutical Sciences, Tokyo University of Science, 2641 Yamazaki, Noda, Chiba 278-8510, Japan.

Received: 17 January 2023 Accepted: 10 August 2023

Published online: 22 August 2023

## References

- Pittenger MF, Mackay AM, Beck SC, et al. Multilineage potential of adult human mesenchymal stem cells. *Science*. 1999;284(5411):143–7.
- Jiang Y, Jahagirdar BN, Reinhardt RL, et al. Pluripotency of mesenchymal stem cells derived from adult marrow. *Nature*. 2002;418(6893):41–9.
- Dominici M, Le Blanc K, Mueller I, et al. Minimal criteria for defining multipotent mesenchymal stromal cells. The international society for cellular therapy position statement. *Cytotherapy*. 2006;8(4):315–7.
- Wu HH, Zhou Y, Tabata Y, Gao JQ. Mesenchymal stem cell-based drug delivery strategy: from cells to biomimetic. *J Control Release*. 2019;294:102–13.
- Takayama Y, Kusamori K, Nishikawa M. Mesenchymal stem/stromal cells as next-generation drug delivery vehicles for cancer therapeutics. *Expert Opin Drug Deliv*. 2021;18(11):1627–42.
- Spees JL, Lee RH, Gregory CA. Mechanisms of mesenchymal stem/stromal cell function. *Stem Cell Res Ther*. 2016;7(1):125.
- Nitzsche F, Müller C, Lukomska B, Jolkonnen J, Deten A, Boltze J. Concise review: MSC adhesion cascade—insights into homing and transendothelial migration. *Stem Cells*. 2017;35(6):1446–60.
- Galderisi U, Peluso G, Di Bernardo G. Clinical trials based on mesenchymal stromal cells are exponentially increasing: where are we in recent years? *Stem Cell Rev Rep*. 2022;18(1):23–36.
- Levy O, Kuai R, Siren EMJ, et al. Shattering barriers toward clinically meaningful MSC therapies. *Sci Adv*. 2020;6(30):eaba6884.
- Kabat M, Bobkov I, Kumar S, Grumet M. Trends in mesenchymal stem cell clinical trials 2004–2018: is efficacy optimal in a narrow dose range? *Stem Cells Transl Med*. 2020;9(1):17–27.

11. Levy O, Kuai R, Siren EMJ, et al. Shattering barriers toward clinically meaningful MSC therapies. *Sci Adv.* 2020;6(30):6884.
12. Kean TJ, Lin P, Caplan AI, Dennis JE. MSCs: delivery routes and engraftment, cell-targeting strategies, and immune modulation. *Stem Cells Int.* 2013;2013: 732742.
13. Krueger TEG, Thorek DLJ, Denmeade SR, Isaacs JT, Brennen WN. Concise review: mesenchymal stem cell-based drug delivery: the good, the bad, the ugly, and the promise. *Stem Cells Transl Med.* 2018;7(9):651–63.
14. van der Helm D, Barnhoorn MC, de Jonge-Muller ESM, et al. Local but not systemic administration of mesenchymal stromal cells ameliorates fibrogenesis in regenerating livers. *J Cell Mol Med.* 2019;23(9):6238–50.
15. Watanabe Y, Tsuchiya A, Seino S, Kawata Y, et al. Mesenchymal stem cells and induced bone marrow-derived macrophages synergistically improve liver fibrosis in mice. *Stem Cells Transl Med.* 2019;8(3):271–84.
16. Armitage JD, Tan DBA, Sturm M, Moodley YP. Transcriptional profiling of circulating mononuclear cells from patients with chronic obstructive pulmonary disease receiving mesenchymal stromal cell infusions. *Stem Cells Transl Med.* 2021;10(11):1470–81.
17. Yao Y, Fan XL, Jiang D, et al. Connexin 43-mediated mitochondrial transfer of iPSC-MSCs alleviates asthma inflammation. *Stem Cell Rep.* 2018;11(5):1120–35.
18. Kikuchi-Taura A, Okinaka Y, Saino O, Takeuchi Y, et al. Gap junction-mediated cell-cell interaction between transplanted mesenchymal stem cells and vascular endothelium in stroke. *Stem Cells.* 2021;39(7):904–12.
19. Fischer UM, Harting MT, Jimenez F, et al. Pulmonary passage is a major obstacle for intravenous stem cell delivery: the pulmonary first-pass effect. *Stem Cells Dev.* 2009;18(5):683–92.
20. Nystedt J, Anderson H, Tikkanen J, et al. Cell surface structures influence lung clearance rate of systemically infused mesenchymal stromal cells. *Stem Cells.* 2013;31(2):317–26.
21. Kerkelä E, Hakkarainen T, Mäkelä T, et al. Transient proteolytic modification of mesenchymal stromal cells increases lung clearance rate and targeting to injured tissue. *Stem Cells Transl Med.* 2013;2(7):510–20.
22. Wang S, Guo L, Ge J, et al. Excess integrins cause lung entrapment of mesenchymal stem cells. *Stem Cells.* 2015;33(11):3315–26.
23. Lee DY, Yang K, Lee S, et al. Optimization of monomethoxy-polyethylene glycol grafting on the pancreatic islet capsules. *J Biomed Mater Res.* 2002;62(3):372–7.
24. Lee DY, Park SJ, Nam JH, Byun Y. A combination therapy of PEGylation and immunosuppressive agent for successful islet transplantation. *J Control Release.* 2006;110:290–5.
25. Teramura Y, Asif S, Ekdahl KN, Gustafson E, Nilsson B. Cell adhesion induced using surface modification with cell-penetrating peptide-conjugated poly(ethylene glycol)-lipid: a new cell glue for 3D cell-based structures. *ACS Appl Mater Interfaces.* 2017;9(1):244–54.
26. Takafuji Y, Higuchi Y, Muro A, et al. Factors influencing the surface modification of mesenchymal stem cells with fluorescein-pegylated lipids. *Biol Pharm Bull.* 2013;36(11):1731–8.
27. Takayama Y, Kusamori K, Hayashi M, et al. Long-term drug modification to the surface of mesenchymal stem cells by the avidin-biotin complex method. *Sci Rep.* 2017;7(1):16953.
28. Kusamori K, Takayama Y, Nishikawa M. Stable surface modification of mesenchymal stem cells using the avidin-biotin complex technique. *Curr Protoc Stem Cell Biol.* 2018;47(1):66.
29. Takayama Y, Kusamori K, Tsukimori C, et al. Anticancer drug-loaded mesenchymal stem cells for targeted cancer therapy. *J Control Release.* 2021;329:1090–101.
30. Shimomura A, Takasaki R, Takayama Y, et al. Intravenous injection of mesenchymal stem cell spheroids improves the pulmonary delivery and prolongs in vivo survival. *Biotechnol J.* 2022;17(1):2100137.
31. Cho KA, Woo SY, Seoh JY, Han HS, Ryu KH. Mesenchymal stem cells restore CCl<sub>4</sub>-induced liver injury by an antioxidative process. *Cell Biol Int.* 2012;36(12):1267–74.
32. Fathi-Kazerooni M, Kazemnejad S, Khanjani S, Saltanatpour Z, Tavosidana G. Down-regulation of miR-122 after transplantation of mesenchymal stem cells in acute liver failure in mice model. *Biologicals.* 2019;58:64–72.
33. Sasaki D, Kusamori K, Takayama Y, Itakura S, Todo H, Nishikawa M. Development of nanoparticles derived from corn as mass producible bionanoparticles with anticancer activity. *Sci Rep.* 2021;11(1):22818.
34. Yukawa H, Watanabe M, Kaji N, et al. Monitoring transplanted adipose tissue-derived stem cells combined with heparin in the liver by fluorescence imaging using quantum dots. *Biomaterials.* 2012;33(7):2177–86.
35. Xue G, Han X, Ma X, et al. Effect of microenvironment on differentiation of human umbilical cord mesenchymal stem cells into hepatocytes in vitro and in vivo. *Biomed Res Int.* 2016;2016:8916534.
36. Saidi R, Rajeshkumar R, Sharifabrizi A, Zimmerman A, Walter O. Human adipose-derived mesenchymal stem cells promote liver regeneration. *J Investig Surg.* 2015;28(6):303–8.
37. Zamperone A, Pietronave S, Merlin S, et al. Isolation and characterization of a spontaneously immortalized multipotent mesenchymal cell line derived from mouse subcutaneous adipose tissue. *Stem Cells Dev.* 2013;22(21):2873–84.
38. Kidd S, Spaeth E, Dembinski JL, et al. Direct evidence of mesenchymal stem cell tropism for tumor and wounding microenvironments using in vivo bioluminescent imaging. *Stem Cells.* 2009;27(10):2614–23.
39. Lanzoni G, Linetsky E, Correa D, et al. Umbilical cord mesenchymal stem cells for COVID-19 acute respiratory distress syndrome: a double-blind, phase 1/2a, randomized controlled trial. *Stem Cells Transl Med.* 2021;10(5):660–73.
40. Karyana M, Djaharuddin I, Rif'ati L, et al. Safety of DW-MSC infusion in patients with low clinical risk COVID-19 infection: a randomized, double-blind, placebo-controlled trial. *Stem Cell Res Ther.* 2022;13(1):134.
41. Yao S, Li X, Liu J, Sun Y, Wang Z, Jiang Y. Maximized nanodrug-loaded mesenchymal stem cells by a dual drug-loaded mode for the systemic treatment of metastatic lung cancer. *Drug Deliv.* 2017;24(1):1372–83.
42. Hatakeyama H, Akita H, Harashima H. A multifunctional envelope type nano device (MEND) for gene delivery to tumours based on the EPR effect: a strategy for overcoming the PEG dilemma. *Adv Drug Deliv Rev.* 2011;63(3):152–60.
43. Noiri M, Asawa K, Okada N, et al. Modification of human MSC surface with oligopeptide-PEG-lipids for selective binding to activated endothelium. *J Biomed Mater Res A.* 2019;107(8):1779–92.
44. Sarkar D, Vemula PK, Teo GS, et al. Chemical engineering of mesenchymal stem cells to induce a cell rolling response. *Bioconjug Chem.* 2008;19(11):2105–9.
45. Sackstein R, Merzaban JS, Cain DW, et al. Ex vivo glycan engineering of CD44 programs human multipotent mesenchymal stromal cell trafficking to bone. *Nat Med.* 2008;14(2):181–7.
46. Cheng H, Byrskas-Bishop M, Zhang CT, et al. Stem cell membrane engineering for cell rolling using peptide conjugation and tuning of cell-selectin interaction kinetics. *Biomaterials.* 2012;33(20):5004–12.
47. Ko IK, Kean TJ, Dennis JE. Targeting mesenchymal stem cells to activated endothelial cells. *Biomaterials.* 2009;30(22):3702–10.
48. Lo CY, Antonopoulos A, Dell A, Haslam SM, Lee T, Neelamegham S. The use of surface immobilization of P-selectin glycoprotein ligand-1 on mesenchymal stem cells to facilitate selectin mediated cell tethering and rolling. *Biomaterials.* 2013;34(33):8213–22.
49. Won YW, Patel AN, Bull DA. Cell surface engineering to enhance mesenchymal stem cell migration toward an SDF-1 gradient. *Biomaterials.* 2014;35(21):5627–35.
50. Dykstra B, Lee J, Mortensen LJ, et al. Glycoengineering of E-selectin ligands by intracellular versus extracellular fucosylation differentially affects osteotropism of human mesenchymal stem cells. *Stem Cells.* 2016;34(10):2501–11.
51. Chou KJ, Lee PT, Chen CL, et al. CD44 fucosylation on mesenchymal stem cell enhances homing and macrophage polarization in ischemic kidney injury. *Exp Cell Res.* 2017;350(1):91–102.
52. Kim JC, Tae G. The modulation of biodistribution of stem cells by anchoring lipid-conjugated heparin on the cell surface. *J Control Release.* 2015;217:128–37.
53. Tatsumi K, Ohashi K, Matsubara Y, et al. Tissue factor triggers procoagulation in transplanted mesenchymal stem cells leading to thromboembolism. *Biochem Biophys Res Commun.* 2013;431(2):203–9.
54. Moll G, Ankrum JA, Kamhieh-Milz J, et al. Intravascular mesenchymal stromal/stem cell therapy product diversification: time for new clinical guidelines. *Trends Mol Med.* 2019;25(2):149–63.
55. Lee DY, Lee S, Nam JH, Byun Y. Minimization of immunosuppressive therapy after islet transplantation: combined action of heme oxygenase-1 and PEGylation to islet. *Am J Transplant.* 2006;6(8):1820–8.

56. Lee DY, Park SJ, Lee S, Nam JH, Byun Y. Highly poly(ethylene) glycolylated islets improve long-term islet allograft survival without immunosuppressive medication. *Tissue Eng.* 2007;13(8):2133–41.
57. Jeong JH, Hong SW, Hong S, et al. Surface camouflage of pancreatic islets using 6-arm-PEG-catechol in combined therapy with tacrolimus and anti-CD154 monoclonal antibody for xenotransplantation. *Biomaterials.* 2011;32(31):7961–70.
58. Stabler CL, Giraldo JA, Berman DM, et al. Transplantation of PEGylated islets enhances therapeutic efficacy in a diabetic nonhuman primate model. *Am J Transplant.* 2020;20(3):689–700.
59. Cinamon G, Alon R. A real time in vitro assay for studying leukocyte transendothelial migration under physiological flow conditions. *J Immunol Methods.* 2003;273(1–2):53–62.
60. Chamberlain G, Smith H, Rainger GE, Middleton J. Mesenchymal stem cells exhibit firm adhesion, crawling, spreading and transmigration across aortic endothelial cells: effects of chemokines and shear. *PLoS ONE.* 2011;6(9):25663.
61. Kang SA, Bajana S, Tanaka T. In vitro flow adhesion assay for analyzing shear-resistant adhesion of metastatic cancer cells to endothelial cells. *Bio Protoc.* 2016;6(4):1731.
62. Giraldo JA, Molano RD, Rengifo HR, Fotino C, Gattás-Asfura KM, Pileggi A, Stabler CL. The impact of cell surface PEGylation and short-course immunotherapy on islet graft survival in an allogeneic murine model. *Acta Biomater.* 2017;49:272–83.
63. Wilson JT, Cui W, Kozlovskaya V, et al. Cell surface engineering with poly-electrolyte multilayer thin films. *J Am Chem Soc.* 2011;133(18):7054–64.
64. Teramura Y, Iwata H. Islets surface modification prevents blood-mediated inflammatory responses. *Bioconjugate Chem.* 2008;19(7):1389–95.
65. Tanaka G, Nakase I, Fukuda Y, et al. CXCR4 stimulates macropinocytosis: implications for cellular uptake of arginine-rich cell-penetrating peptides and HIV. *Chem Biol.* 2012;19(11):1437–46.
66. Galleu A, Riffo-Vasquez Y, Trento C, et al. Apoptosis in mesenchymal stromal cells induces in vivo recipient-mediated immunomodulation. *Sci Transl Med.* 2017;9(416):7828.
67. Pang SHM, D’Rozario J, Mendonca S, et al. Mesenchymal stromal cell apoptosis is required for their therapeutic function. *Nat Commun.* 2021;12(1):6495.
68. Wu HJ, Yiu WH, Wong DWL, et al. Human induced pluripotent stem cell-derived mesenchymal stem cells prevent adriamycin nephropathy in mice. *Oncotarget.* 2017;8(61):103640–56.
69. He Z, Hua J, Qian D, et al. Intravenous hMSCs ameliorate acute pancreatitis in mice via secretion of tumor necrosis factor- $\alpha$  stimulated gene/protein 6. *Sci Rep.* 2016;6:38438.

## Publisher’s Note

Springer Nature remains neutral with regard to jurisdictional claims in published maps and institutional affiliations.

Ready to submit your research? Choose BMC and benefit from:

- fast, convenient online submission
- thorough peer review by experienced researchers in your field
- rapid publication on acceptance
- support for research data, including large and complex data types
- gold Open Access which fosters wider collaboration and increased citations
- maximum visibility for your research: over 100M website views per year

At BMC, research is always in progress.

Learn more [biomedcentral.com/submissions](https://biomedcentral.com/submissions)

